

# Physical mechanism of surface roughening on the radial core-shell nanowire heterostructure with alloy shell

Yuanyuan Cao and Dongfeng Diao

Citation: *AIP Advances* **7**, 055006 (2017); doi: 10.1063/1.4983577

View online: <http://dx.doi.org/10.1063/1.4983577>

View Table of Contents: <http://aip.scitation.org/toc/adv/7/5>

Published by the [American Institute of Physics](#)

---

## Articles you may be interested in

[Highly efficient isolation of waterborne sound by an air-sealed meta-screen](#)

*AIP Advances* **7**, 055001 (2017); 10.1063/1.4983035

[Cautions to predicate multiferroic by atomic force microscopy](#)

*AIP Advances* **7**, 055003 (2017); 10.1063/1.4983271

[TEM EDS analysis of epitaxially-grown self-assembled indium islands](#)

*AIP Advances* **7**, 055005 (2017); 10.1063/1.4983492

[Field synergy characteristics in condensation heat transfer with non-condensable gas over a horizontal tube](#)

*AIP Advances* **7**, 055101 (2017); 10.1063/1.4979329

[Effect of crystallinity on UV degradability of poly\[methyl\(phenyl\)silane\] by energy-resolved electrochemical impedance spectroscopy](#)

*AIP Advances* **7**, 055002 (2017); 10.1063/1.4983215

[Radial tunnel diodes based on InP/InGaAs core-shell nanowires](#)

*Applied Physics Letters* **110**, 113501 (2017); 10.1063/1.4978271

---

# HAVE YOU HEARD?

Employers hiring scientists and engineers trust

**PHYSICS TODAY | JOBS**

[www.physicstoday.org/jobs](http://www.physicstoday.org/jobs)



## Physical mechanism of surface roughening on the radial core-shell nanowire heterostructure with alloy shell

Yuanyuan Cao and Dongfeng Diao<sup>a</sup>

*Institute of Nanosurface Science and Engineering (INSE), Guangdong Provincial Key Laboratory of Micro/Nano Optomechatronics Engineering, Shenzhen University, Shenzhen 518060, China*

(Received 24 March 2017; accepted 3 May 2017; published online 11 May 2017)

We proposed a quantitative thermodynamic theory to address the physical process of surface roughening during the epitaxial growth of core-shell NW with alloy layer. The surface roughening originates from the transformation of the Frank-van der Merwe (FM) mode to the Stranski-Krastanow (SK) mode. In addition to the radius of NW core, the composition and thickness of alloy shell could determine the growth behaviors due to their modulation to the strain. The established theoretical model not only explains the surface roughening caused by the alloy shell layer, but also provides a new way to control the growth of core-shell NW. © 2017 Author(s). All article content, except where otherwise noted, is licensed under a Creative Commons Attribution (CC BY) license (<http://creativecommons.org/licenses/by/4.0/>). [<http://dx.doi.org/10.1063/1.4983577>]

The radial core-shell nanowire (NW), especially the Si-core/Ge-shell NW structure, has attracted considerable interest, as a result of the potential for advanced microelectronic and optoelectronic nanodevices, such as sensors,<sup>1</sup> solar cells,<sup>2</sup> and transistors,<sup>3</sup> due to the tunable band gaps and increased charge carrier mobility.<sup>4–6</sup> However, the surface roughening, which exhibited as a periodic modulation with island-like morphologies, would always appear on the surface of core-shell NW. Although surface roughening can be considered as a quantum dot (QD)-NW heterostructure,<sup>7</sup> it is a major obstacle to the epitaxial growth of high quality core-shell NW experimentally,<sup>8–10</sup> because it would destroy the core-shell structure. Fortunately, Si-core/Ge-shell NW has already been realized on thin NW experimentally.<sup>10–12</sup> However, if the diameter of NW becomes larger, Ge QD would appear on NW.<sup>8,11–13</sup> Similarly, the other systems, such as GaAs/InAs,<sup>14</sup> InAs/InP,<sup>15</sup> GaAs/AlGaAs system,<sup>16</sup> InAs/GaSb,<sup>17</sup> and AlAs/GaAs,<sup>18</sup> have the same growth behaviors. Thus, the diameter of NW plays an important role in determining the surface roughening. However, modulating the core-shell NW by limiting the diameter of NW would impede the further development of core-shell NW devices, and cannot resolve the puzzle of surface roughening thoroughly.

In addition to the diameter of NW, the shell constitute can also control the appearance of surface roughening, such as taking the  $\text{Si}_x\text{Ge}_{1-x}$  alloy layer instead of pure Ge materials growing on Si NW.<sup>19</sup> Furthermore, the alloy shell can also improve the optical properties due to the composition features.<sup>20</sup> However, owing to the join of alloy shell, the growth mechanism of core-shell NW is more complex. The theoretical works on the core-shell NW have developed from the thermodynamic energy analysis of NW and the epitaxial growth behavior to the physical origin of the surface roughening on core-shell NW.<sup>21–26</sup> Our previous theoretical model<sup>26</sup> have studied the epitaxial growth of core-shell NW with single-element shell layer, and only focused on the effect of NW diameter. However, the underlying physical mechanism involved in the surface roughening of core-shell NW with alloy shell is still unclear. Thus, it is urgent to investigate the basic physics involved in the epitaxial growth of core-shell NW heterostructure with alloy shell.

In this contribution, by accounting for the influence of alloy shell layer, we propose a quantitative thermodynamic theory to address the epitaxial growth of core-shell NW heterostructure. Taking

<sup>a</sup>Corresponding author: [dfdiao@szu.edu.cn](mailto:dfdiao@szu.edu.cn)

Si-core/Si<sub>x</sub>Ge<sub>1-x</sub>-shell NW structure as an example, we reveal that the composition and thickness of the shell layer determines the surface roughening on core-shell NW.

On the basis of the physical origin of surface roughening, the smooth shell layer growth on NW can be considered as a layer by layer growth (Frank-van der Merwe, FM mode) on a curved surface, while the surface roughening can be attributed to the QD formation (Stranski-Krastanow, SK mode) on the NW. The surface stability of core-shell NW is decided by the energy competition of the two growth modes. Assuming a two-dimensional epitaxial Si<sub>x</sub>Ge<sub>1-x</sub> layer with thickness  $t_{WL}$  on the Si NW with radius of  $R_{NW}$ , the composition of Si in the epitaxial alloy layer is  $x$ . The energy difference caused by unit volume  $\Delta V$  of atoms diffusing from the layer to QD is

$$\Delta E = E_{SK} - E_{FM} \quad (1)$$

where  $E_{SK}$  is the energy change of QD with increased unit volume  $\Delta V$ , while  $E_{FM}$  is the energy change when the layer added unit volume  $\Delta V$ . In order to minimize the total energy of the whole system and achieve the stable state, the system needs to be under the condition of  $\Delta E = 0$ . If  $\Delta E < 0$ , the growth of QD will be favorable, while the layer will grow thicker when  $\Delta E > 0$ .

Considering the influence of the content of Si in Si<sub>x</sub>Ge<sub>1-x</sub> alloy layer, the strain of the alloy layer on a plan substrate can be considered as  $\varepsilon_a = \frac{1-x}{1-x\varepsilon_0} \varepsilon_0$ , where  $\varepsilon_0 = \frac{a_{shell} - a_{NW}}{a_{shell}}$ .  $a_{NW}$  and  $a_{shell}$  are the lattice constants of the bulk material of the NW and the single-element shell layer. Furthermore, because the NW surface is curved, the strain between the epitaxial layer and the NW becomes more complex than that on planar substrate. In the longitudinal direction, because of the minor effect of the curved surface, the strain component is similar to the epitaxial growth on the planar substrate as  $\varepsilon_z = \varepsilon_a$ . In the direction normal to the NW surface, there is no stress by omitting the effect of the two ends of the NW.<sup>27</sup> Also, the shear strain components are all equal to zero.<sup>28</sup> The contribution of curvature is mainly acted on the tangential direction to the NW surface. The tangential strain  $\varepsilon_t$  has a relationship with the radius of NW  $R_{NW}$  and the thickness of layer  $t$ ,<sup>21</sup> and can be expressed as  $\varepsilon_t(t) = \varepsilon_a - \frac{t}{R_{NW}}(1 - \varepsilon_a)$ . Therefore, the average strain is  $\varepsilon = (\varepsilon_a + \varepsilon_t)/2$ .

Based on the surface strain of the alloy layer on NW with different thickness, we can decide the strain energy of the shell layer as

$$E_{FM}^{el} = 2Gi \frac{(1+\nu)}{1-\nu} \Delta V \frac{\int_{R_{NW}+t_{WL}}^{R_{NW}+t_{WL}+\Delta t} \varepsilon(r)^2 r dr}{\int_{R_{NW}+t_{WL}}^{R_{NW}+t_{WL}+\Delta t} r dr}. \quad (2)$$

Moreover, the surface energy would change with the volume, and can be written as

$$E_{FM}^s = \frac{\Delta V}{\rho_c} \left[ \frac{(\gamma_a - \gamma_{NW})}{h_o} e^{-\frac{t_{WL}}{h_o}} + \frac{\gamma_{WL}}{R_{NW} + t_{WL}} \right]. \quad (3)$$

The first term reflects the influence of layer thickness, in which  $h_o$  is the thickness of the monolayer,  $\gamma_a$  and  $\gamma_{NW}$  represent the surface energy density of the bulk material of alloy layer and NW, respectively. Meanwhile, the last term shows the effect of the surface curvature on the change of surface energy.  $\gamma_{WL}$  is the energy surface density with thickness of  $t_{WL} + \Delta t$ , which we can express as  $\gamma_{WL} = \gamma_{NW} + (\gamma_a - \gamma_{NW})(1 - e^{-\frac{t_{WL}+\Delta t}{h_o}})$ .<sup>29,30</sup>  $\Delta t$  is the increment thickness of the wetting layer with  $\Delta V$  atoms transferred. The relationship between  $\Delta t$  and  $\Delta V$  is  $\Delta t = \rho_c \Delta V$ , where  $\rho_c$  is the density of the QDs. Therefore, according to the elastic strain energy and the surface energy, the energy change of the epitaxial layer caused by the atoms migrating is

$$E_{FM} = E_{FM}^{el} + E_{FM}^s. \quad (4)$$

Meanwhile, the migration of atoms would lead to the energy change of QD, including the surface energy, strain energy and strain relaxation energy. When unit volume of atoms adding to the QD, the surface energy change of single QD is

$$E_{SK}^s = \frac{\zeta \gamma_a - \xi \gamma_{WL}}{r_{island}} \Delta V, \quad (5)$$

in which  $\zeta$  and  $\xi$  are the shape factors of the QD. Note that, the QD can form until the volume achieves the critical volume, thus  $r_{island}$  is the radius of the QD with critical volume.<sup>21,31,32</sup> Furthermore, based

on the strain dependent on layer thickness, the elastic strain energy of QD must be integral with different layers in the QD, which can be expressed as

$$E_{SK}^{el} = 2Gi \frac{1 + \nu}{1 - \nu} \Delta V \frac{\int_0^{h_{island}} \varepsilon(h)^2 (h_{island} - h)^2 dh}{\int_0^{h_{island}} (h_{island} - h)^2 dh}, \quad (6)$$

where  $h_{island}$  is the height of the QD with critical volume,  $Gi$  and  $\nu$  are the shear modulus and Poisson ratio. However, the strain not only affects the elastic strain energy of QD, but also the elastic relaxation energy. The elastic relaxation energy drives the formation of QD, which can be calculated by

$$E_{SK}^r = -\kappa Y \frac{1 + \nu}{1 - \nu} \tan \alpha \Delta V \frac{\int_0^{h_{island}} \varepsilon(h)^2 (h_{island} - h)^2 dh}{\int_0^{h_{island}} (h_{island} - h)^2 dh}, \quad (7)$$

in which  $Y$  is the Young's modulus,  $\kappa$  is the numerical shape factor and  $\alpha$  is the contact angle of the QD. Based on the surface energy, elastic strain and relaxation energy, the total energy change of QD induced by the added volume is

$$E_{SK} = E_{SK}^{el} + E_{SK}^r + E_{SK}^s. \quad (8)$$

Therefore, we can obtain the energy difference  $\Delta E$  caused by  $\Delta V$  of atoms diffusing from the layer to QD. We can judge whether the surface roughening appears by comparing the energy change of the layer and the QD. When  $E_{SK} > E_{FM}$ , the layer growth is preferred, that is, the core-shell NW structure can be well presented. Contrarily, when  $E_{SK} < E_{FM}$ , the surface roughening phenomena will appear.

To check the validity of our model, we used the Si-core/Si<sub>x</sub>Ge<sub>1-x</sub>-shell NW structure as an example in this study. In order to illustrate the growth mechanism of the core-shell NW with alloy shell, we studied the epitaxial growth on planar substrate firstly as showed in Fig. 1(a). That is Si-core/Si<sub>x</sub>Ge<sub>1-x</sub>-shell NW with infinite radius of NW. The black line represents the pure Ge epitaxial layer growth on Si substrate. With few epitaxial layers on the substrate, the energy change of FM mode is smaller than the SK mode because the layer can store all the strain. Thus, the FM growth mode, which is represented by PF1, is favorable. However, the layer cannot withstand the energy when the layer thickens to a critical thickness. Then QD would form to release the energy, i.e. SK growth mode denoted by PS1 appears. The results are in good agreement with Ge epitaxial layer growth on Si planar substrate both in theory and experiments.<sup>21,33-35</sup> When Ge epitaxial layer changes to be Si<sub>x</sub>Ge<sub>1-x</sub> alloy layer, the strain would decrease with the Si composition  $x$ . Hence, the alloy layer grows thicker than the pure Ge layer due to the decreasing energy in every layer. Taking  $x = 0.3$  as the example, the critical thickness which divides the FM mode (PF2) and SK mode (PS2) is thicker than  $x = 0$ . Furthermore, the critical thickness increases with the composition  $x$ . If the composition of Si continues to increase, the strain would be small enough to store in the layer rather than forming QD. Then the FM growth mode is more favorable than the SK mode no matter how thick the layers are. In the example of  $x = 0.6$ , the energy difference between the two modes is always above the zero line. Thus, there is only FM mode, which is represented by PF3.

On the basis of the epitaxial growth on planar substrate, we studied the influence of alloy layer on the epitaxial growth of core-shell NW. Figs. 1(b) and 1(c) show the results of Si-core/Si<sub>x</sub>Ge<sub>1-x</sub>-shell NW structure with radius of 30 nm and 10 nm, respectively. Comparing with the planar substrate, the shell layers release more strain and the change in surface area becomes larger due to the curvature of NW substrate. However, the pure Ge epitaxial layer growth on NWs with radius of 30 nm and 10 nm both converts from FM to SK. The FM and SK mode are represented by NF1 and NS1 respectively. With the composition of Si increases, such as  $x = 0.3$ , the strain decreases. Hence, the shell layer thickens when the growth mode transform from FM to SK during the initial layer deposited. The two growth modes are represented by NF2 and NS2. However, for the thinner NW with radius of 10 nm, the curvature of NW is large enough to relax the strain to the minimum when the shell layer continues to thicken. Then the shell layer can release the strain rather than forming QDs, thus the growth mode turns back to FM mode again, which has been observed experimentally.<sup>11</sup> The second FM mode is represented by NF2-B. When the composition increases to be 0.6, for the thicker NW with radius of 30 nm, the strain achieves a minimum state, and the critical thickness of shell layer corresponding to

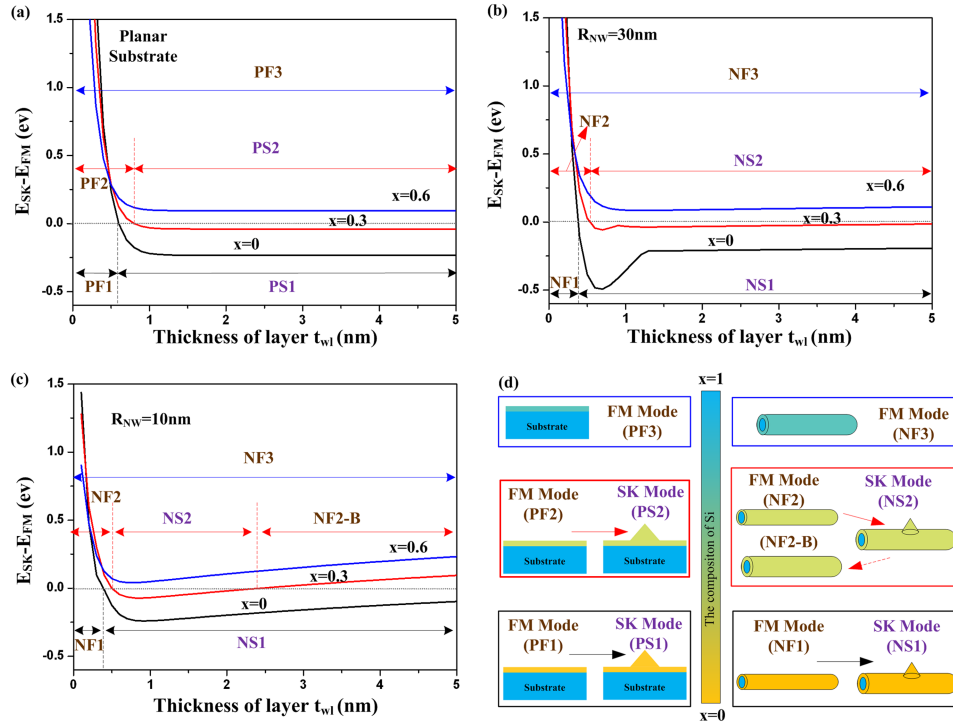


FIG. 1. The energy difference between the two growth modes as the function of epitaxial layer thickness on planar substrate (a) and NW substrate with radius of 30 nm (b) and 10 nm (c). The black, red and blue line represent  $\text{Si}_x\text{Ge}_{1-x}$  alloy shell with composition  $x = 0, 0.3, 0.6$ , respectively. (d) Schematic illustration of FM and SK growth modes on planar substrate and NW substrate. The blue degree denotes the composition of Si in  $\text{Si}_x\text{Ge}_{1-x}$  alloy shell. PF and PS represent FM modes and SK modes on planar substrate with different composition, while NF and NS denote FM modes and SK modes on NW substrate.

the transition to the SK mode increases to infinite. Then the shell layer can store all the energy and the surface of core-shell NW keeps stable no matter how thick the shell layer is. For the thinner NW with radius of 10 nm, the SK mode region between the two critical thickness reduces until disappear with the composition increase as showed in Fig. 1(c). Hence, there is only FM mode (NF3) without the limitation of shell scale and NW radius when the composition is large enough.

Fig. 1(d) shows the schematic illustration of the growth mode transformation. The left parts illustrate the FM mode (PF1, PF2, PF3) and SK mode (PS1, PS2) of alloy layer with composition  $x = 0, x = 0.3$ , and  $x = 0.6$  growth on planar substrate. The right parts illustrate the modes transition on NW substrate. The growth mode on NWs with radius of 30 nm and 10 nm transforms from FM (NF1) to SK (NS1) when  $x = 0$ . When the composition increases to 0.3, the FM mode (NF2) still transforms to SK mode (NS2), but the FM mode (NF2-B) appears again on thinner NW substrate. When the composition is large enough, the effect of radius becomes negligible. There is always FM mode which is illustrated by NF3. Therefore, we can conclude that the composition of shell layer plays an important role to control the occurrence of surface roughening on core-shell NW.

According to the analysis above, the radius of NW core, the thickness and the composition of alloy shell layer all play important roles in determining the epitaxial growth modes. Fig. 2 shows the diagram of the surface roughening on the core-shell NW with the radius of NW core and the composition of shell when the layer thickness is 3 nm. Due to the decreased strain caused by the curvature of NW, thinner NW could be more stable with the same shell layer. Moreover, the surface roughening on the larger NW could disappear by increasing the composition, because larger composition can decrease the strain directly. The critical line, which represents the largest radius for core-shell NW without surface roughening, divides the regime into the SK mode and FM mode in Fig. 2. The purple region above the critical line enables the formation of QD while the FM mode becomes favorable in the yellow region. In experiments, Si-core/Ge-shell NW has been synthesized with radius between 5 nm-7.5 nm,<sup>10,11</sup> while surface roughening appears on larger NW, such as the experimental data

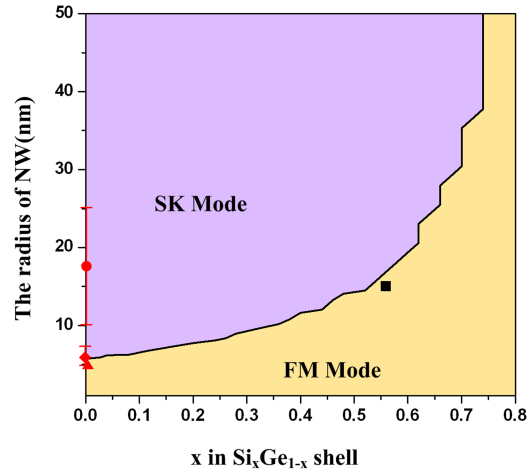


FIG. 2. Phase diagram of surface roughening on the Si-core/ $\text{Si}_x\text{Ge}_{1-x}$ -shell NW with the composition  $x$  of alloy shell and the radius of NW. The purple region enables the formation of QD, while FM mode is favorable in yellow region. The experimental data ( $\blacklozenge$   $\blacktriangle$   $\blacksquare$ ) of core-shell NW in yellow region are from refs. 10, 11, and 19, respectively. The experimental data ( $\bullet$ ) in purple region is from ref. 13.

in purple region.<sup>13</sup> Furthermore, Si-core/ $\text{Si}_{0.56}\text{Ge}_{0.44}$ -shell NW have been realized with radius of 15 nm,<sup>19</sup> which is in good agreement with our theoretical model. Hence, modulating composition of shell layer can widen the scale range of core-shell NW without surface roughening.

In order to illustrate the effect of the alloy shell layer clearly, we conclude the phase diagram of the surface roughening on the NW with radius of 15 nm based on the composition and the thickness of shell layer as showed in Fig. 3. In the left part of the diagram where the composition is smaller, the ability of the layer to store energy is limited and the strain could decrease by thickening the curved layer. Hence, the thickness of shell layer plays a major role in controlling the surface roughening. With the composition increases, the effect of composition in decreasing the strain becomes more effectively than the layer thickness. Thus, the FM mode is favorable again because the larger composition and the thicker shell layer decrease the strain to the minimum. Meanwhile, if the composition continues to increase, the strain is small enough to be stored in the shell layer rather than relaxed by forming QD. Hence, the FM mode is always preferred without the limitation of layer thickness. Importantly, the Si-core/ $\text{Si}_x\text{Ge}_{1-x}$ -shell NWs have been realized with 3.9 nm  $\text{Si}_{0.39}\text{Ge}_{0.61}$  alloy shell layer and

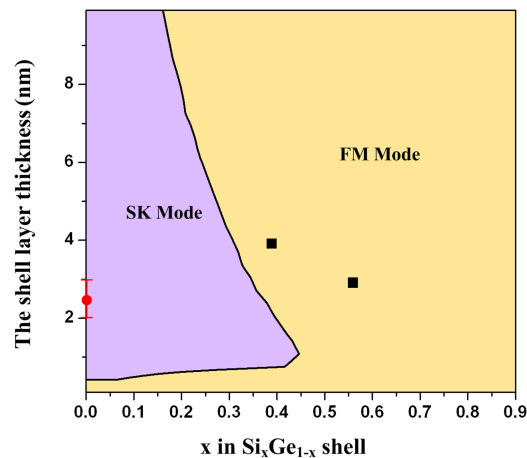


FIG. 3. Phase diagram of surface roughening on the Si-core/ $\text{Si}_x\text{Ge}_{1-x}$ -shell NW with the composition  $x$  and the thickness of the alloy shell layer. The surface roughening would appear on core-shell NW in the purple region while stable core-shell NW can be obtained in yellow region. The experimental data ( $\blacksquare$ ) in the yellow region which denote the perfect core-shell NW are from ref. 19, while the experimental data ( $\bullet$ ) of core-shell NW with surface roughening are from ref. 13.

2.9 nm  $\text{Si}_{0.56}\text{Ge}_{0.44}$  alloy shell layer experimentally,<sup>19</sup> which are both located in the yellow region. Meanwhile, with the same radius of 15 nm, the surface of Si-core/Ge-shell NW always appear roughening in experiments,<sup>13</sup> which is in good agreement with our theoretical results.

In summary, we have developed a quantitative thermodynamic model to address the physical mechanism of the epitaxial growth of the radial core-shell NW structure with alloy shell. The competition of the FM and SK mode can determine the surface roughening. In addition to the radius of NW core, the composition and the thickness of the alloy shell layer are important factors to control the growth behavior. Furthermore, modulating alloy shell can not only break the scale limitation in avoiding the surface roughening, but also apply more possibility to the epitaxial growth of core-shell NW. Importantly, the agreement between the theoretical results and experiments for the radial Si-core/ $\text{Si}_x\text{Ge}_{1-x}$ -shell NW structure suggests that the developed model is applicable to the understanding and design of epitaxial growth on core-shell NW.

The authors would like to thank the National Nature Science Foundation of China (No. 11404217) and Shenzhen Fundamental Research subject-layout project (JCYJ20160427105015701).

- <sup>1</sup> Y. J. Hu, H. O. H. Churchill, D. J. Reilly, J. Xiang, C. M. Lieber, and C. M. Marcus, *Nat. Nanotechnology* **2**, 622 (2007).
- <sup>2</sup> B. Tian, X. Zheng, T. J. Kempa, Y. Fang, N. Yu, G. Yu, J. Huang, and C. M. Lieber, *Nature* **449**, 885 (2007).
- <sup>3</sup> L. Chen, F. Cai, U. Otuonye, and W. D. Lu, *Nano Lett.* **16**, 420 (2016).
- <sup>4</sup> K. B. Dhungana, M. Jaishi, and R. Pati, *Nano Lett.* **16**, 3995 (2016).
- <sup>5</sup> J. Xiang, W. Lu, Y. Hu, H. Yan, and C. M. Lieber, *Nature* **441**, 489 (2006).
- <sup>6</sup> M. Amato, S. Ossicini, and R. Rural, *Nano Lett.* **11**, 594 (2011).
- <sup>7</sup> Y. Jung, D. K. Ko, and R. Agarwal, *Nano Lett.* **7**, 264 (2007).
- <sup>8</sup> L. Pan, K.-K. Lew, J. M. Redwing, and E. C. Dickey, *Nano Lett.* **5**, 1081 (2005).
- <sup>9</sup> I. A. Goldthorpe, A. F. Marshall, and P. C. McIntyre, *Nano Lett.* **9**, 3715 (2009).
- <sup>10</sup> L. J. Lauhon, M. S. Gudiksen, D. Wang, and C. M. Lieber, *Nature* **420**, 57 (2002).
- <sup>11</sup> B.-M. Nguyen, B. Swartzentruber, Y. G. Ro, and S. A. Dayeh, *Nano Lett.* **15**, 7258 (2015).
- <sup>12</sup> Y. Pan, G. Hong, S. N. Raja, S. Zimmermann, M. K. Tiwari, and D. Poulidakos, *Appl. Phys. Lett.* **106**, 093102 (2015).
- <sup>13</sup> S. Kwon, Z. C. Y. Chen, J.-H. Kim, and J. Xiang, *Nano Lett.* **12**, 4757 (2012).
- <sup>14</sup> K. L. Kavanagh, J. Salfi, I. Savelyev, M. Blumin, and H. E. Ruda, *Appl. Phys. Lett.* **98**, 152103 (2011).
- <sup>15</sup> C. M. Haapamaki, J. Baugh, and R. R. LaPierre, *J. Cryst. Growth* **345**, 11 (2012).
- <sup>16</sup> Q. Zhang, J.-N. Aqua, P. W. Voorhees, and S. H. Davis, *J. Mech. Phys. Solids* **91**, 73 (2016).
- <sup>17</sup> X. Ji, X. Yang, W. Du, H. Pan, S. Luo, H. Ji, H. Q. Xu, and T. Yang, *Nanotechnology* **27**, 275601 (2016).
- <sup>18</sup> A. Li, D. Ercolani, L. Lugani, L. Nasi, F. Rossi, G. Salviati, F. Beltram, and L. Sorba, *Cryst. Growth Des.* **11**, 4053 (2011).
- <sup>19</sup> D. C. Dillen, F. Wen, K. Kim, and E. Tutuc, *Nano Lett.* **16**, 392 (2016).
- <sup>20</sup> N. Jeon, B. Loitsch, S. Morkoetter, G. Abstreiter, J. Finley, H. J. Krenner, G. Koblmüller, and L. J. Lauhon, *ACS Nano* **9**, 8335 (2015).
- <sup>21</sup> X. L. Li, C. X. Wang, and G. W. Yang, *Progress in Materials Science* **64**, 121 (2014).
- <sup>22</sup> X. L. Li, *Nanotechnology* **25**, 185702 (2014).
- <sup>23</sup> V. Schmidt, P. C. McIntyre, and U. Gösele, *Phys. Rev. B* **77**, 235302 (2008).
- <sup>24</sup> H. Wang, M. Upmanyu, and C. V. Ciobanu, *Nano Lett.* **8**, 4305 (2008).
- <sup>25</sup> N. S. Mohammad, *J. Phys.: Condens. Matter* **26**, 423202 (2014).
- <sup>26</sup> Y. Y. Cao, G. Ouyang, C. X. Wang, and G. W. Yang, *Nano Lett.* **13**, 436 (2013).
- <sup>27</sup> H. Wang, M. Upmanyu, and C. V. Ciobanu, *Nano Lett.* **8**, 4305 (2008).
- <sup>28</sup> S. Raychaudhuri and E. T. Yu, *J. Appl. Phys.* **99**, 114308 (2006).
- <sup>29</sup> Y. Y. Cao and G. W. Yang, *Appl. Phys. Lett.* **95**, 231902 (2009).
- <sup>30</sup> X. L. Li, *Applied Surface Science* **256**, 4023 (2010).
- <sup>31</sup> X. L. Li, *J. Phys. Chem. C* **114**, 2018 (2010).
- <sup>32</sup> X. L. Li, *Phys. Chem. Chem. Phys.* **15**, 5238 (2013).
- <sup>33</sup> J. Tersoff, *Phys. Rev. B* **43**, 9377 (1991).
- <sup>34</sup> O. G. Schmidt, O. Kienzle, Y. Hao, K. Eberl, and F. Ernst, *Appl. Phys. Lett.* **74**, 1272 (1999).
- <sup>35</sup> A. Vailionis, B. Cho, G. Glass, P. Desjardins, D. G. Cahill, and J. E. Greene, *Phys. Rev. Lett.* **85**, 3672 (2000).